High-fat diet decreases cancellous bone mass but has no effect on cortical bone mass in the tibia in mice ☆

Jay J. Cao [a,*], Brian R. Gregoire [a], Hongwei Gao [b]

[a] USDA, Agricultural Research Service, Grand Forks Human Nutrition Research Center 2420 2nd Ave N Grand Forks, ND 58202-9034, USA
[b] Center for Experimental Therapeutics and Reperfusion Injury, Department of Anesthesia Perioperative and Pain Medicine, Brigham and Women's Hospital and Harvard Medical School, Boston, MA 02115, USA

ARTICLE INFO

ABSTRACT

Body mass has a positive effect on bone health. Whether mass derived from an obesity condition or excessive fat accumulation is beneficial to bone has not been established; neither have the mechanisms by which obesity affects bone metabolism. The aim of this study was to examine the effects of obesity on bone structure and osteoblastic expression of key markers involved in bone formation and resorption in a diet-induced obesity mouse model. Six-wk-old male C57BL/6 mice ($n = 21$) were assigned to two groups and fed either a control (10 kcal% energy as fat) or high-fat diet (HFD, 45 kcal% energy as fat) for 14 weeks. Bone marrow stromal/osteoblastic cells (BMSC) were cultured. Osteoprogenitor activity [alkaline phosphatase (ALP) positive colonies] and mineralization (calcium nodule formation) were determined. Gene expression was measured using quantitative real-time PCR. Bone structure of proximal and midshaft tibia was evaluated by micro-computed tomography. Mice fed the HFD were 31% heavier ($P < 0.01$) than those fed the control diet. There were more ALP positive colony forming units at d 14 and calcium nodules at d 28 of culture by BMSC from HFD mice than from control mice ($P < 0.01$). Receptor activator of NF-κB ligand (RANKL) mRNA levels and the ratio of RANKL to osteoprotegerin expression in HFD animals was higher ($P < 0.01$) than in control diet animals. Serum tartrate-resistant acid phosphatase levels were higher in HFD fed mice when compared to control diet fed mice ($P < 0.05$). There were no significant differences in tibial fat-free weight, length, and cortical parameters of midshaft between the two groups. Compared with control mice, tibial trabecular bone volume was reduced, and trabecular separation was increased in HFD mice. Trabecular number was lower ($P < 0.05$) and connectivity density tended to be less ($P = 0.07$) in HFD mice than in control mice. In conclusion, our data indicate that obesity induced by a high-fat diet decreases cancellous bone mass but has no effect on cortical bone mass in the tibia in mice.

Published by Elsevier Inc.

Introduction

Despite being a risk factor for many chronic health disorders, obesity, a major public health problem affecting more than 300 million people globally, has been thought beneficial to bone and a protective factor for osteoporosis in humans [1–3]. Any effects alleged to be beneficial to bone are mainly based on a well-established positive correlation between body weight (BW) (or mechanical loading conferred by BW) and bone mineral density (BMD) found in animals and humans [4–6]. Mechanical loading stimulates bone formation by decreasing apoptosis and increasing proliferation and differentiation of osteoblasts and osteocytes [7] possibly through Wnt/β-catenin signaling pathway [8,9]. However, accumulating data suggest that excessive fat mass is detrimental to bone [10–12]. Marrow adipogenesis may be inversely related to osteoblastogenesis since adipocyte and bone-forming cell, osteoblast, are derived from a common multi-potential mesenchymal stem cell [13,14].

In a genetic mouse model for obesity, leptin-deficient (ob/ob) mice weighed twice as much as lean mice and but had lower femoral BMD, cortical thickness, and trabecular bone volume [15]. Apparently the positive effect of mechanical loading conferred by body weight could not overcome the detrimental effect of obesity (or possibly leptin deficiency) on bone in these mice.

In diet-induced obesity animal studies, structure and mechanical properties of both cortical and cancellous bones were negatively affected by diets with high fat content [16,17]. When fed a high-fat diet (HFD) for two years, rats had a significantly smaller average cross-sectional area of the sixth lumbar vertebra and lower loads, energies, and stiffness of both L6 and femoral neck when these parameters were

adjusted to body mass [18]. However, none of these studies evaluated bone structure with micro-CT tomography (μCT) technology or addressed possible mechanisms by which HFD affects bone metabolism.

We evaluated bone architecture of proximal and midshaft tibia by μCT in mice fed a HFD for 14 wks to determine whether a HFD influences bone structure. To determine the HFD on functions of osteoblasts, we cultured bone marrow stromal/osteoblastic cells (BMSC) for up to 28 days. The number and area of alkaline phosphatase positive colony forming units (CFU-ALP$^+$) at d 14 and calcium nodules at d 28 were measured in addition to the expression of ALP, alpha 1 collagen (COL1A1), osteocalcin (OC), receptor activator of NF-κB ligand (RANKL), osteoprotegerin (OPG), and macrophage colony stimulation factor (M-CSF).

Materials and methods

Chemicals and reagents

Ketamine HCl was purchased from Animal Health Co. (St. Joseph, MO). Xylazine HCl was purchased from Phoenix Scientific (St. Joseph, MO). Fetal bovine serum (FBS) was from Atlanta Biologicals (Nocross, GA). The following reagents and kits were purchased from Sigma-Aldrich (St. Louis, MO): Alpha modified essential medium (αMEM), tartrate-resistant acid phosphatase (TRAP) staining kit, Alizarin Red (A5533) and ALP staining kit (86R). Trizol reagent was purchased from Invitrogen (Carlsbad, CA). The oligonucleotide primers for PCR amplification were designed by the Primer Express software (Version 3.0) from Applied Biosystems (Foster City, CA) and synthesized by Integrated DNA Technologies (IDT, Coralville, IA) with HPLC purification.

Animals and diets

Male C57BL/6 mice, 6 wks old, were obtained from Charles River Laboratories. All mice were housed in Plexiglas ventilated cages (2 animals/cage) with alpha-dri bedding within a pathogen-free facility that maintained a 12-hour light/12-hour dark cycle. The animal protocol for the study was approved by the USDA-ARS Grand Forks Human Nutrition Research Center Animal Care Committee. Animals were maintained and processed in accordance with the NIH Guide for the Care and Use of Laboratory Animals. Mice were allowed to acclimate in our animal facility for 3 days before being randomly assigned into two groups ($n = 11$ for the control group and $n = 10$ for the HFD group).

Mice had free access to tap water throughout the study. During the study, mice consumed ad libitum either a control purified diet (Control, 10% energy as fat, D12450B, New Brunswick, NJ) based on AIN-93G [19] or a HFD (45% energy as fat) with extra fat from lard for 14 wks (Table 1). Body weight was recorded weekly.

Preparation of bones and measurements of fat-free weight and midshaft diameter

Mice were euthanized with a ketamine cocktail (1.37:1 mixture of ketamine:xylazine). Both tibias and femurs of each mouse were removed and cleaned of adherent tissue. For fat-free weight (FFW), the tibias were defatted by sequential extraction in ethanol and diethyl ether using a Soxhlet apparatus. After drying overnight at 95 °C, bones were weighed and their length and midshaft diameter were measured using a Max Cal Digital Caliper (Fre V. Fowler Co. Inc., Newton, MA) before being submitted to μCT scans as described below.

BMSC cultures

For the marrow harvest, one tibia and one femur from each mouse were briefly immersed in 70% ethanol (3 s), and stored in primary medium (α-MEM containing L-glutamine, nucleosides, supplemented with 10% FBS, 1% penicillin–streptomycin, and 0.1% fungizone) temporarily before BMSC were isolated and cultured as outlined below. The bones were rinsed four times (2 min each) in a calcium- and magnesium-free PBS (PBS-CMF) containing antibiotics (penicillin–streptomycin) and fungizone under sterile conditions. The epiphyses of each bone were removed with a razor blade and discarded. The marrow was flushed out from the diaphysis with a syringe and 26.5-gauge needle, and collected in primary culture medium. The marrow cell suspension was gently drawn through an 18-gauge needle to mechanically dissociate the mixture into a single cell suspension. The cells were plated at 10×10^6 cells/10 cm tissue culture dish. On day 5, nonadherent cells were removed by aspiration, and adherent cells (osteoblast-like cells) were replenished with secondary medium (primary medium sup-plemented with 50 μg/ml L-ascorbic acid and 3 mM β-glycerophosphate) to induce mesenchymal cells to form osteoblasts. Subsequent media changes were performed every 2 days for up to 28 days.

Determination of CFU-ALP$^+$ and calcium nodule formation

At 14 days of culture, cells were washed twice with PBS-CMF and fixed in 10% formalin for 1 h then washed twice with distilled H_2O. Alkaline phosphatase positive colony forming units were stained with a commercially available kit. At 28 days of culture, plates containing BMSC were rinsed with PBS-CMF and fixed for 1 h with 10% formalin. After fixed cultures were rinsed with distilled H_2O, they were stained with 2% Alizarin red (AR) for 10 min and rinsed five times with distilled H_2O to remove loosely bound stain to reveal mineralized colonies. The number and area of CFU-ALP$^+$ colonies and calcium nodules more than 1 mm in diameter were counted and measured with an imaging analyzer (Image Pro 4.5, Media Cybernetics, Inc., Bethesda, MD).

Measurement of mRNA levels in BMSC

BMSC were washed with PBS-CMF twice and collected for RNA isolation at 14 days of culture. Total RNA was extracted using Trizol

Table 1
Composition of experimental diets[a].

Ingredient	Control	High-fat diet
		g
Casein, 80 Mesh	200	200
L-Cystine	3	3
Corn starch	315	72.8
Maltodextrin 10	35	100
Sucrose	350	172.8
Cellulose, BW200	50	50
Soybean oil	25	25
Lard	20	177.5
Mineral mix[b]	10	10
Dicalcium phosphate	13	13
Calcium carbonate	5.5	5.5
Potassium citrate, 1H2O	16.5	16.5
Vitamin mix[c]	10	10
Choline bitartrate	2	2
Total weight, g	1055	858
Energy, kcal/g diet	3.85	4.73
% Energy		
Carbohydrate	70	35
Protein	20	20
Fat	10	45

[a] Prepared by Research Diet, Inc., New Brunswick, NJ.
[b] The mineral mix composition was as follows (amount in 10 g): 0.5 g Mg, 0.3 g S, 1.0 g Na, 1.6 g Cl, 6.0 mg Cu, 0.2 mg I, 45.0 mg Fe, 59 mg Mn, 0.2 mg Se and 29 mg Zn.
[c] The vitamin mix composition was as follows (amount in 10 g): 4000 IU vitamin A palmitate, 1000 IU cholecalciferol, 50 IU vitamin E acetate, 0.5 mg menadione sodium bisulfite, 0.2 mg biotin, 10 μg cyanocobalamin, 2 mg folic acid, 30 mg nicotinic acid, 16 mg calcium pantothenate, 7 mg pyridoxine-HCl, 6 mg riboflavin, 6 mg thiamin HCl.

reagent according to the manufacturer's protocol. Denatured total RNA from cells (2 µg) was reverse transcribed with the following components from Applied Biosystems: 1× reverse transcription buffer, 5.5 mM mgCl$_2$, 500 µM of each dNTPs, 2.5 µM random hexamers, 0.4 U/µl of RNase inhibitor, and 1.25 U/µl MultiScribe reverse transcription enzyme in a 100-µl reaction volume with the following protocol: hexamer incubation at 25 °C for 10 min, reverse transcription at 37 °C for 1 h, and heat inactivation of reverse transcriptase at 95 °C for 5 min.

The levels of mRNA of ALP, COL1A1, OC, RANKL, OPG, and M-CSF were determined by qPCR. The sequence information of oligonucleo-tide primers is presented in Table 2. Following reverse transcription, the cDNA (2 µl) was amplified and quantified using a Sequence Detection System (SDS 7300) and a PCR universal protocol as follows: AmpliTaq Gold activation at 95 °C for 15 s and, annealing/extension at 60 °C for 1 min. The fluorescence of the double-stranded products accumulated was monitored in real time. The relative mRNA levels were normalized to levels of GAPDH mRNA in the same sample.

To confirm the specificity of our primers and to ensure that samples were free of DNA contamination, RT-PCR products were run for dissociation curve. Only one distinct peak was observed for each gene (data not shown).

Serum TRAP5b measurement

The mouse TRAP assay kit was purchased from Immunodiagnostic System (Fountain Hill, AZ). Serum TRAP5b was determined according to the manufacturer's instructions.

Micro computed tomography measurements

The influence of dietary fat on trabecular and cortical bone microstructure was assessed at the tibial proximal metaphysis and mid-diaphysis. The tibia was placed in a holder of 10.2-mm in diameter and scanned using a Scanco µCT scanner (µCT-40; Scanco Medical AG, Bassersdorf, Switzerland) at 6 µm isotropic voxel size with X-ray source power of 55 kV and 145 µA and integration time of 300 ms. The scans for trabecular bone were initiated from the growth plate cross-sectionally and moving distally for a total of 400 slices and for assessment of cortical parameters a scan of 60 slices was performed for each bone [20–22]. The grey-scale images were processed using a low-pass Gaussian filter (sigma = 0.8, support = 1) to remove noise, and a fixed threshold of 220 was used to extract the mineralized bone from soft tissue and marrow phase. The reconstruction and 3D quantitative analyses were performed by using software provided by Scanco. The same settings for scan and analysis were used for all samples.

A direct three dimension (3D) evaluation of trabecular bone structural parameters was done in a region of interest (ROI) that consisted of about 120 slices starting from about 0.1 mm distal to growth plate, constituting 0.70 mm in length. Cancellous bone was separated from the cortical regions by semi-automatically drawn contours. The following 3D parameters in the defined ROI were analyzed: bone volume (BV, mm^3), tissue (cortical and marrow) volume (TV, mm^3), relative bone volume over total volume (BV/TV, %), trabecular number (Tb.N, 1/mm), trabecular thickness (Tb.Th, µm), trabecular separation (Tb.Sp, µm), connectivity density (Conn.Dn, 1/mm^3), structure model index (SMI, ranges from 0 to 3 with 0 = platelike and 3 = rodlike), and BMD (g hydroxyapatite/cm^3). BMD is the average density of the segmented fraction of the ROI (bone) not including the marrow cavity. The ROI of cortical analyses consisted about 60 slices that cover the length of 0.24 mm at the tibial midshaft. The following cortical parameters in the defined ROI were calculated and averaged at the cross-slide defined as the midpoint between the proximal and distal epiphyses: cortical thickness (Ct.Th, mm), bone area (B.Ar, mm^2), and medullary area (Me.Ar, mm^2). Bone histomorphometry nomenclature follows recommended standards [23].

Data Analysis

Data on all parameter are expressed as group means ± SE ($n = 10$–11 animals/group). Differences between the experimental groups were analyzed using the Student t-Test. Differences between groups at different time-points (body weights) were analyzed by repeated measurement of analysis of covariance (ANCOVA) using baseline weight as the covariate (SAS version 9.1.3, SAS Institute, Inc., Cary, NC) [24]. In all of the analyses, $P < 0.05$ was considered to be statistically significant.

Results

Body weight

The body weight at each time point for the two groups is shown in Fig. 1. Starting from five wks of age, the body weight of animals fed the HFD was significantly greater than that of mice fed the control diet

Table 2
Oligonucleotide primers for cDNA amplification[a].

Oligonucleotide	GeneBank accession no.	Sequence (5′–3′)	Amplicon length	Corresponding cDNA sequence
AP forward primer	J02980	TCCTGACCAAAAACCTCAAAGG	101	1138–1159
AP reverse primer		TGCTTCATGCAGAGCCTGC		1238–1220
OC forward primer	U11542	CTCACAGATGCCAAGCCC	98	76–93
OC reverse primer		CCAAGGTAGCGCCGGAGTCT		173–154
COL1A1 forward primer	U08020	GCGAAGGCAACAGTCGCT	101	4166–4183
COL1A1 reverse primer		CTTGGTGGTTTTGTATTCGATGAC		4266–4243
GAPDH forward primer	XM 001473623.1	TGCACCACCAACTGCTTAG	177	520–538
GAPDH reverse primer		GGATGCAGGGATGATGTTC		696–678
RANKL forward primer	AF053713	CCTGAGGCCCAGCCATTT	108	644–661
RANKL reverse primer		CTTGGCCCAGCCTCGAT		751–735
OPG forward primer	U94331	TACCTGGAGATCGAATTCTGCTT	110	424–446
OPG reverse primer		CCATCTGGACATTTTTTGCAAA		533–512
M-CSF forward primer	NM_007778	CATCCACGCTGCCGTGAAG	62	1567–1584
M-CSF reverse primer		GGGATTCGGTGTCGCAATAT		1628–1609

[a] The oligonucleotide primers for PCR amplification were designed by the Primer Express software (Version 3.0) from Applied Biosystems and synthesized by Integrated DNA Technologies (IDT, Coralville, IA) with HPLC purification. The specificity of primers was confirmed by running dissociation curse with Sequence Detection System (SDS 7300).

($P<0.05$). From this time on, the difference between the two groups increased constantly. At the end of the study (14 wks on experimental diets), mice on the HFD weighed about 31% heavier than control mice (31 ± 1 and 41 ± 2 g for control and HFD mice, respectively).

BMSC differentiation

To determine the effect of dietary fat on bone marrow stromal/osteoblastic cell differentiation, osteoprogenitor number, and mineralization, we cultured BMSC from tibias and femurs *in vitro* and measured the number and area of CFU-ALP$^+$ at d 14 and mineralizing nodules at d 28 of culture (Fig. 2). Compared with mice fed the control diet, HFD fed mice had significantly increased ($P<0.01$) the number of CFU-ALP$^+$ colonies at d 14 of culture (93 ± 11 vs 143 ± 9 for control and HFD mice, respectively) (Fig. 2B). The total area of these CFU-ALP$^+$ colonies (Fig. 2C) was greater ($P<0.01$) for the HFD group than the control group (436 ± 65 vs 649 ± 73 mm^2, respectively). When cultured *in vitro* under differentiating reagents (vitamin C and β-glycerophosphate), BMSC started to form mineralizing nodules at d 21 of culture and maximal calcium nodules were observed at d 28 of culture. At d 28 of culture, the number of AR-stained calcium nodules (Fig. 2B) was increased ($P<0.01$) in BMSC from mice fed the HFD compared with mice fed the control diet (45 ± 11 vs 90 ± 7 for control and HFD mice, respectively). Mice on the HFD were associated with a significant 2.2-fold increase in the total area of mineralizing nodules compared with mice on the control diet (Fig. 2C).

Expression of ALP, COL1A1, OC, RANKL, and OPG in osteoblastic cells

To determine the effect of the HFD on the expression of markers of osteoblasts, we measured ALP, COL1A1, and OC mRNA levels in BMSC by quantitative real-time PCR (Fig. 3). All values were normalized to GAPDH mRNA levels and expressed as a percentage of the controls. Compared with the control diet, the HFD increased ($P<0.05$) ALP mRNA levels by 41% (Fig. 3A). No differences were found in COL1A1 and OC mRNA levels in BMSC between the two groups at d 14 of culture (Fig. 3A).

To determine the effect of the HFD on the expression of genes involved in bone resorption process, we measured mRNA levels for RANKL, OPG, and M-CSF in BMSC (Fig. 3B). At 14 days after plating, RANKL mRNA levels in BMSC from HFD mice were higher ($P<0.05$) than those from control mice (Fig. 3B). Differences were not detected in OPG mRNA levels in BMSC from HFD mice as compared to that from
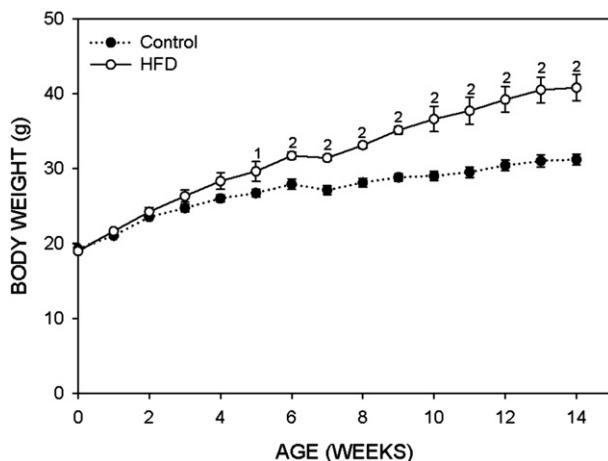
Fig. 1. Changes in body weight of mice fed the control diet (Control) and the high-fat diet (HFD) for 14 wks. Results are mean ± SE ($n=11$ for the control group and $n=10$ for the HFD group). Data were analyzed by one-way ANCOVA with repeated measures. [1]$P<0.05$ and [2]$P<0.01$ compared to the control group.
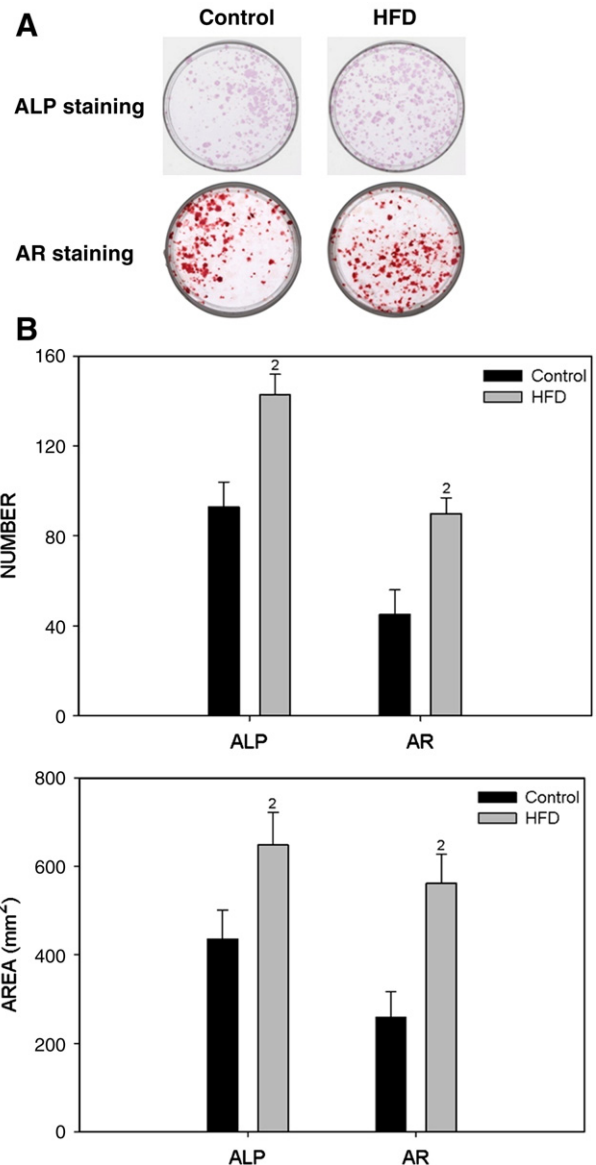
Fig. 2. Determination of alkaline phosphatase positive colony forming units (CFU-ALP$^+$) and calcium nodules in bone marrow stromal/osteoblastic cell (BMSC) culture. (A) Representative plates of BMSC culture at d 14 of culture stained for alkaline phosphatase activity (ALP) and at d 28 of culture for Alizarin Red (AR) stained mineralizing nodules. The number (B) and total area (C) of CFU-ALP$^+$ colonies and calcium nodules that were >1 mm in diameter were counted and measured with an imaging analyzer (Image Pro 4.5, Media Cybernetics). Data are mean ± SE ($n=11$ for the control group and $n=10$ for the HFD group). [2]$P<0.01$ compared with mice fed the control diet, Student *t*-Test.

control mice ($P>0.05$) (Fig. 3B). As a result, the ratio of RANKL to OPG expression in HFD animals was higher ($P<0.01$) than in control diet animals (data not shown). No differences ($P>0.05$) were found in M-CSF mRNA levels between HFD and control mice (Fig. 3B).

Serum TRAP levels

Consistent with the increased RANKL expression in cultured osteoblasts, the levels of serum TRAP (Fig. 4), a marker of bone resorption, were higher in HFD mice when compared to control mice (7.0 ± 0.4 vs 10.24 ± 1.3 U/L for control and HFD mice, respectively).

Bone mass and structure

The FFW and the length of the tibia are reported in Table 3. While body weight of HFD mice increased by about 31% compared with
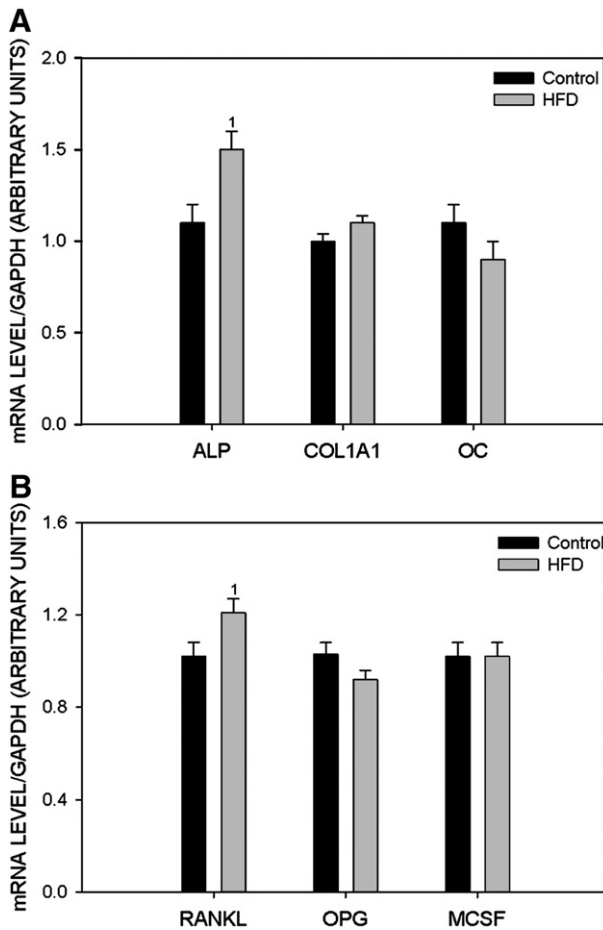
Fig. 3. Gene expression levels in bone marrow stromal/osteoblastic cells (BMSC) at d 14 of culture in mice fed the control and the high-fat diet (HFD) as measured by quantitative real-time PCR. (A) Alkaline phosphatase (ALP), alpha 1 collagen (COL1A1), and osteocalcin (OC). (B) Receptor activator of NF-κB ligand (RANKL), osteoprotegerin (OPG), and macrophage colony stimulation factor (M-CSF). Data are mean ± SE ($n = 11$ for the control group and $n = 10$ for the HFD group). [1]$P < 0.05$ compared with mice fed the control diet, Student t-Test.

control mice at the end of study (Fig. 1), no difference ($P > 0.05$) was found in FFW of mice fed the HFD compared with mice fed the control diet. However, when adjusted for body weight, FFW of control mice (1.24 ± 0.04 mg/g) was significantly greater than FFW/BW of HFD mice (0.97 ± 0.03 mg/g; $P < 0.01$). Diets had no effect ($P > 0.05$) on either tibial length or midshaft diameter of mice.

Non-destructive μCT was used to evaluate the effect of diets on bone structure in proximal (Fig. 5) and midshaft (Table 3) tibia. Total bone area was the same in HFD as in control mice (Table 3). Significant differences in cortical measurements (Ct.Th, B.Ar, and Me.Ar) were not detected between control and HFD mice. Examination of proximal tibia revealed that trabecular bone was affected by the HFD (Fig. 5). While the TV was not different between two groups, the tibial BV of HFD mice was significantly lower than that of control mice ($P < 0.05$). As a result, HFD mice had about 5% lower BV/TV than control mice (20.6 vs. 15.8% for control and HFD mice, respectively; $P < 0.05$). Compared to mice fed the control diet, trabecular thickness was not significantly different between two groups but trabecular number was lower ($P < 0.05$) in HFD mice than in control animals. Trabecular separation increased significantly in HFD mice compared to control mice (185 ± 7 and 213 ± 11 μm for control and HFD mice, respectively; $P < 0.05$). Mice fed the HFD diet had marginally less connectivity density than those fed the control diet (166 ± 9 and 132 ± 16 1/mm^3 for control and HFD mice, respectively; $P = 0.07$). Structural model index was not significantly altered by the HFD for the proximal tibia
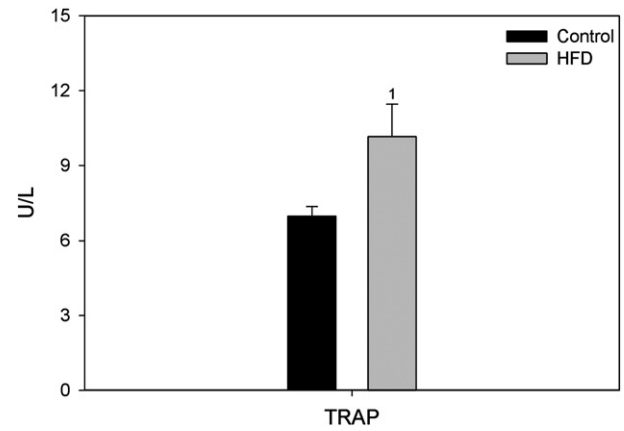
Fig. 4. Serum tartrate-resistant acid phosphatase (TRAP) concentration in mice fed the control and the high-fat diet (HFD). Data are mean ± SE ($n = 11$ for the control group and $n = 10$ for the HFD group). [1]$P < 0.05$ compared with mice fed the control diet, Student t-Test.

(Fig. 5F). No changes in segmented BMD were detected between HFD and control mice (Fig. 5G).

Discussion

In the present study we have shown that feeding mice a high-fat diet (45% energy as fat) for 14 wks decreases trabecular bone volume and trabecular number in the proximal tibia but has no effect on cortical bone mass despite a substantial increase in body weight and bone formation markers in cultured BMSC in a diet-induced obesity mouse model. These structural changes are accompanied by increases in serum TRAP levels and the ratio of RANKL/OPG expression in cultured osteoblasts.

The C57BL/6 mice were used as a model in our study since the skeletal structure changes with age in these animals are similar to those that occur in humans [22]. Furthermore, the diet-induced obesity mouse shares many features of human obesity and metabolic syndrome. When fed a high-fat diet, animals develop central adiposity, hyperinsulinemia, insulin resistance, hyperglycemia, and hypertension [25,26]. As expected, mice on the HFD are obese and accumulated much abdominal fat (our own observation); therefore they were much heavier than those on the normal-fat diet.

Bone marrow stromal cells or osteoprogenitors can be differentiated into osteoblast-like cells through several phases: proliferation, organic matrix synthesis, and matrix mineralization when cultured in α-MEM media supplemented with vitamin C and β-glyceralphosphate. Each phase is accompanied by the sequential expression of various genes considered to be osteoblast markers. Alkaline phosphatase is an early osteoblast differentiation marker and is associated with organic bone matrix synthesis before its mineralization. Our *in vitro* culture of BMSC

Table 3
Fat-free weight, length of whole tibia and structural parameters of midshaft tibia in mice fed the control and the high-fat diet.

	Control	HFD	P value
Whole tibia			
Fat-free weight (mg)	38.9 ± 1.4	39.3 ± 2.0	0.868
Length (mm)	17.8 ± 0.1	17.8 ± 0.1	0.416
Midshaft tibia			
Diameter (mm)	1.00 ± 0.02	1.01 ± 0.02	0.716
Ct.Th (mm)	0.22 ± 0.01	0.21 ± 0.01	0.641
B.Ar (mm^2)	0.71 ± 0.03	0.68 ± 0.03	0.545
Me.Ar (mm^2)	0.46 ± 0.02	0.48 ± 0.02	0.275
Total bone area (mm^2)	1.17 ± 0.04	1.17 ± 0.04	0.275

Values are means ± SE. Control diet (Control): 10% energy as fat, High-fat diet (HFD): 45% energy as fat. Significant differences were assessed by the Student's t-Test.
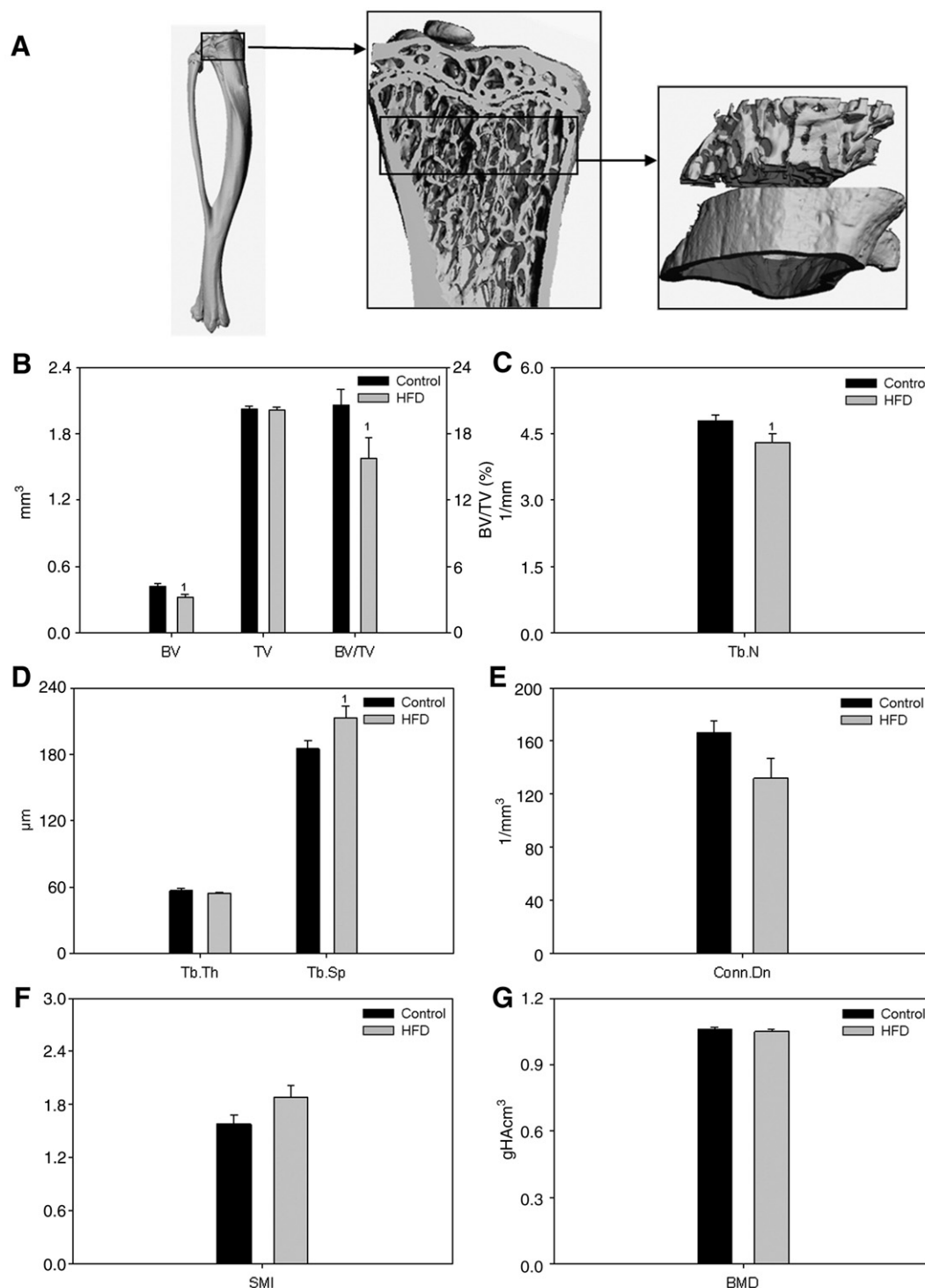
Fig. 5. Structural parameters of the trabecular bone of the proximal tibia in mice fed the control and the high-fat diet (HFD). (A) The figures illustrate the region of a tibia of a mouse analyzed by μCT. The trabecular bone can be separated from cortical bone and analyzed with this technology. An evaluation of trabecular bone structural parameters was done in a region of interest that consisted of 120 slices starting from approximately 0.1 mm distal to growth plate, constituting 0.72 mm in length. (B) Bone volume (BV) and tissue volume (TV). (C) Trabecular number (Tb.N). (D) Trabecular thickness (Tb.Th) and trabecular separation (Tb.Sp). (E) Connectivity density (Conn. Dn). (F) Structural model index (SMI). (G) Bone mineral density (BMD). Data are mean ± SE ($n = 11$ for the control group and $n = 10$ for the HFD group). [1]$P < 0.05$ compared with mice fed the control diet, Student t-Test.

demonstrated that the number and proliferative potential of osteoprogenitors were increased in mice fed the HFD compared to those fed the control diet as evidenced by the number and total area of alkaline phosphatase positive colonies and alkaline phosphatase mRNA expression in BMSC at d 14 (Figs. 2A–C). These results combined with the increase in the formation of mineralizing nodules (AR staining) suggest that bone formation may be increased in mice fed HFD although it remains to be determined *in vivo*. It is well known that biomechanical

loading of body weight stimulates bone formation, decreases apoptosis and increases proliferation and differentiation of osteoblasts and osteocytes [7] while reduced loading due to hindlimb unloading or microgravity conditions induces significant bone loss, inhibits the proliferation and differentiation of osteoprogenitor cells and decreases osteoblast number and maturation [7,27,28]. Therefore the finding of increased bone formation markers in our study is not surprising, considering HFD mice weighed considerably more than controls.

The HFD did not affect fat-free weight, length, and midshaft diameter of the tibia, a finding similar to few other studies where bone morphology was evaluated [16,29,30]. The developmental growth of mice may or may not be affected by the HFD. Or these parameters are not sensitive to reflect the difference in developmental growth. Excessive fat mass accumulation was likely the main attributing factor to the body weight gain in mice on the HFD [18,26,29,31]. Serum concentrations of hormones related to developmental growth, such as GH or IGF-I were not measured in the present study. Other studies have shown that these hormones would not be affected in rats by HFD [31] or markedly blunted in obese human subjects [32]. On the other hand, evidence suggested that high circulating concentrations of leptin in obesity can stimulate skeletal growth [33].

There was no difference in BMD (material not including the marrow cavity) of either cancellous or cortical bone between the two diet groups, indicating that high-fat diet did not impair mineralization. Contrary to the finding of increased bone formation markers in cultured osteoblasts, we found that obese mice had lower tibial trabecular bone volume and lower trabecular number, and greater trabecular separation than control mice, suggesting that bone resorption might be increased in HFD animals.

The finding of HFD being detrimental to bone structure in the tibia is in agreement with some reports where different species and evaluation methods were used [16–18,34]. Our results differ with Smith et al. who reported that the HFD did not affect bone size, composition or mechanical properties in rats where animals were fed the HFD for only two weeks [30]. Although Brahmabhatt et. al. concluded that the weight gain produced by DIO may lead to improved biomechanics (such as ultimate load and femoral energy absorption capacity) in rats, they also showed that the ash content of both cortical and cancellous bone was lower for rats termed "gainers" whose body weights were 19% heavier than controls, which is similar to our findings [29]. Differences in animal species, dietary fat levels, and duration of high-fat feeding may account for some of the inconsistent conclusions. Moreover, none of these studies used μCT technology to evaluate bone structure at different sites. We scanned the bones with the highest resolution (6 μm) to evaluate bone architecture non-destructively in our DIO mouse model. Higher resolution would allow a more accurate estimate of the bone structure.

Cortical parameters (B.Ar, Ct.Th, and Me.Ar) were not affected by the HFD diet. The finding of cancellous rather than cortical bone affected by the HFD is not surprising. In general, cancellous bone is more responsive than cortical bone to diet or drug treatments, physiological status, or aging because the cancellous bone is more actively remodeled than cortical bone due to the larger surface to volume ratio [35]. Other possible explanations are that midshaft cortical bone might not have enough time to adapt the way of macromodeling, or bone geometry at the midshaft did not change due to biochemical and/or endocrinological constraints imposed by the fat:lean ratio, or geometry changes did not reflect the additional weight of obese mice. Had our data been adjusted to body weight as was done in another study [18], a HFD would have decreased all cortical bone parameters.

The findings that the high-fat diet adversely affected trabecular bone structure seemed contrary to reports in humans that body mass index is positively associated with BMD [1,4,5]. While mechanical loading conferred by body weight, in no doubt, has positive effect on bone formation, whether excessive fat mass is beneficial to bone or a protective factor for osteoporosis as some have suggested [36] has been questioned. Accumulating data suggest that excessive fat mass is negatively associated with bone mass [10–12]. Determining the effect of obesity on bone health in humans has proved to be difficult because human obesity is a complex issue which involves not only excessive fat intake but also possibly disproportionate consumption of other nutrients, such as protein and minerals, known to influence bone metabolism [37]. Conclusions regarding the relationship between

obesity and bone in humans have mostly relied on statistical correlation or modeling rather than controlled trials. Therefore, the obese mouse animal model is useful for studying the effect of obesity induced by high-fat diet on bone metabolism. Studies have shown that obese animals eat the same amount of energy regardless of dietary fat content [31,38,39]. Therefore, the intake of fat is different while the intake of other nutrients remains the same for HFD mice compared to control mice when a diet formulated on an energy basis (i.e. HFD has a greater nutrient density than the control diet). However, we cannot exclude the possibility that nutrient intake might be different slightly between the two groups. In humans, excess weight in the form of fat mass has been found to be negatively related to radial cortical bone area, total bone cross-sectional area, and cortical bone mineral content in adolescent females [12]. We started a high-fat diet at 6-wk, a time which corresponds to childhood and adolescence. Whether a high-fat diet has similar detrimental effects on bones of mature animals when peak bone mass and strength have been achieved remains to be determined.

Bone is a dynamic organ that undergoes significant turnover, a process called modeling and remodeling which involves bone resorption by osteoclasts followed by bone formation by osteoblasts [40]. Therefore, bone mass reflects the balance of bone formation and resorption. At the cellular level it involves the coordinated regulation of osteoblast and osteoclast number and activity [41]. RANKL/RANK/OPG signaling pathway plays an important role in this regulation. Obesity is associated with a state of chronic inflammation [42,43] and elevated production of pro-inflammatory cytokines, including TNF-α, IL-1β, and IL-6. These cytokines have been shown capable of stimulating osteoclast activity through regulating RANKL/RANK/OPG pathway [44,45]. To further elucidate the possible mechanism by which HFD affects bone structure and cell functions, we measured serum TRAP concentration and mRNA levels of RANKL, OPG and M-CSF in cultured osteoblasts [46–48]. The increased RANKL expression and the ratio of RANKL to OPG in cultured osteoblasts from HFD mice combined with increased serum TRAP levels, suggesting that osteoclast activity and bone resorption are presumably enhanced with HFD.

In conclusion, our results show that obesity induced by feeding a high-fat diet for 14 wks is detrimental to trabecular bone structure in the proximal tibia of young mice. The dramatic increase in body weight of obese mice may favor bone formation but obesity may also increase bone resorption. High-fat diet may alter the balance of bone modeling/remodeling resulting in decreased cancellous bone mass.

Conflict of interest

There are no conflicts of interest.

References

[1] Reid IR, Ames R, Evans MC, Sharpe S, Gamble G, France JT, Lim TM, Cundy TF. Determinants of total body and regional bone mineral density in normal postmenopausal women—a key role for fat mass. J Clin Endocrinol Metab 1992;75:45–51.
[2] Kopelman PG. Obesity as a medical problem. Nature 2000;404:635–43.
[3] Villareal DT, Apovian CM, Kushner RF, Klein S. Obesity in older adults: technical review and position statement of the American Society for Nutrition and NAASO, the Obesity Society. Am J Clin Nutr 2005;82:923–34.
[4] Felson DT, Zhang Y, Hannan MT, Anderson JJ. Effects of weight and body mass index on bone mineral density in men and women: the Framingham study. J Bone Miner Res 1993;8:567–73.
[5] Ravn P, Cizza G, Bjarnason NH, Thompson D, Daley M, Wasnich RD, McClung M, Hosking D, Yates AJ, Christiansen C, Early Postmenopausal Intervention Cohort (EPIC) study group. Low body mass index is an important risk factor for low bone mass and increased bone loss in early postmenopausal women. J Bone Miner Res 1999;14:1622–7.
[6] Robling AG, Castillo AB, Turner CH. Biomechanical and molecular regulation of bone remodeling. Annu Rev Biomed Eng 2006;8:455–98.

[7] Ehrlich PJ, Lanyon LE. Mechanical strain and bone cell function: a review. Osteoporos Int 2002;13:688–700.

[8] Bonewald LF, Johnson ML. Osteocytes, mechanosensing and Wnt signaling. Bone 2008;42:606–15.

[9] Sawakami K, Robling AG, Ai M, Pitner ND, Liu D, Warden SJ, Li J, Maye P, Rowe DW, Duncan RL, Warman ML, Turner CH. The Wnt co-receptor LRP5 is essential for skeletal mechanotransduction but not for the anabolic bone response to parathyroid hormone treatment. J Biol Chem 2006;281:23698–711.

[10] Zhao LJ, Jiang H, Papasian CJ, Maulik D, Drees B, Hamilton J, Deng HW. Correlation of obesity and osteoporosis: effect of fat mass on the determination of osteoporosis. J Bone Miner Res 2008;23:17–29.

[11] Blum M, Harris SS, Must A, Naumova EN, Phillips SM, Rand WM, Dawson-Hughes B. Leptin, body composition and bone mineral density in premenopausal women. Calcif Tissue Int 2003;73:27–32.

[12] Pollock NK, Laing EM, Baile CA, Hamrick MW, Hall DB, Lewis RD. Is adiposity advantageous for bone strength? A peripheral quantitative computed tomography study in late adolescent females. Am J Clin Nutr 2007;86:1530–8.

[13] David V, Martin A, Lafage-Proust MH, Malaval L, Peyroche S, Jones DB, Vico L, Guignandon A. Mechanical loading down-regulates peroxisome proliferator-activated receptor gamma in bone marrow stromal cells and favors osteoblasto-genesis at the expense of adipogenesis. Endocrinology 2007;148:2553–62.

[14] Takada I, Suzawa M, Matsumoto K, Kato S. Suppression of PPAR transactivation switches cell fate of bone marrow stem cells from adipocytes into osteoblasts. Ann N Y Acad Sci 2007;1116:182–95.

[15] Hamrick MW, Pennington C, Newton D, Xie D, Isales C. Leptin deficiency produces contrasting phenotypes in bones of the limb and spine. Bone 2004;34:376–83.

[16] Li KC, Zernicke RF, Barnard RJ, Li AF. Effects of a high fat-sucrose diet on cortical bone morphology and biomechanics. Calcif Tissue Int 1990;47:308–13.

[17] Wohl GR, Loehrke L, Watkins BA, Zernicke RF. Effects of high-fat diet on mature bone mineral content, structure, and mechanical properties. Calcif Tissue Int 1998;63:74–9.

[18] Zernicke RF, Salem GJ, Barnard RJ, Schramm E. Long-term, high-fat-sucrose diet alters rat femoral neck and vertebral morphology, bone mineral content, and mechanical properties. Bone 1995;16:25–31.

[19] Reeves PG, Nielsen FH, Fahey Jr GC. AIN-93 purified diets for laboratory rodents: final report of the American Institute of Nutrition ad hoc writing committee on the reformulation of the AIN-76A rodent diet. J Nutr 1993;123:1939–51.

[20] Droke EA, Hager KA, Lerner MR, Lightfoot SA, Stoecker BJ, Brackett DJ, Smith BJ. Soy isoflavones avert chronic inflammation-induced bone loss and vascular disease. J Inflamm (Lond) 2007;4:17.

[21] Lane NE, Yao W, Nakamura MC, Humphrey MB, Kimmel D, Huang X, Sheppard D, Ross FP, Teitelbaum SL. Mice lacking the integrin beta5 subunit have accelerated osteoclast maturation and increased activity in the estrogen-deficient state. J Bone Miner Res 2005;20:58–66.

[22] Halloran BP, Ferguson VL, Simske SJ, Burghardt A, Venton LL, Majumdar S. Changes in bone structure and mass with advancing age in the male C57BL/6J mouse. J Bone Miner Res 2002;17:1044–50.

[23] Parfitt AM, Drezner MK, Glorieux FH, Kanis JA, Malluche H, Meunier PJ, Ott SM, Recker RR, Report of the ASBMR Histomorphometry Nomenclature Committee. Bone histomorphometry: standardization of nomenclature, symbols, and units. J Bone Miner Res 1987;2:595–610.

[24] SAS Institute Inc.. SAS/STAT User's Guide. Cary, NC: SAS Institute Inc.; 2005.

[25] Surwit RS, Kuhn CM, Cochrane C, McCubbin JA, Feinglos MN. Diet-induced type II diabetes in C57BL/6J mice. Diabetes 1988;37:1163–7.

[26] Collins S, Martin TL, Surwit RS, Robidoux J. Genetic vulnerability to diet-induced obesity in the C57BL/6J mouse: physiological and molecular characteristics. Physiol Behav 2004;81:243–8.

[27] Sakata T, Halloran BP, Elalieh HZ, Munson SJ, Rudner L, Venton L, Ginzinger D, Rosen CJ, Bikle DD. Skeletal unloading induces resistance to insulin-like growth factor I on bone formation. Bone 2003;32:669–80.

[28] Kostenuik PJ, Halloran BP, Morey-Holton ER, Bikle DD. Skeletal unloading inhibits the in vitro proliferation and differentiation of rat osteoprogenitor cells. Am J Physiol 1997;273:E1133–9.

[29] Brahmabhatt V, Rho J, Bernardis L, Gillespie R, Ziv I. The effects of dietary-induced obesity on the biomechanical properties of femora in male rats. Int J Obes Relat Metab Disord 1998;22:813–8.

[30] Smith EE, Ferguson VL, Simske SJ, Gayles EC, Pagliassotti MJ. Effects of high fat or high sucrose diets on rat femora mechanical and compositional properties. Biomed Sci Instrum 2000;36:385–90.

[31] Brown JL, Spicer MT, Spicer LJ. Effect of high-fat diet on body composition and hormone responses to glucose tolerance tests. Endocrine 2002;19:327–32.

[32] Scacchi M, Pincelli AI, Cavagnini F. Growth hormone in obesity. Int J Obes Relat Metab Disord 1999;23:260–71.

[33] Maor G, Rochwerger M, Segev Y, Phillip M. Leptin acts as a growth factor on the chondrocytes of skeletal growth centers. J Bone Miner Res 2002;17:1034–43.

[34] Atteh JO, Leeson S, Julian RJ. Effects of dietary levels and types of fat on performance and mineral metabolism of broiler chicks. Poult Sci 1983;62:2403–11.

[35] Morgan EF, Barnes GL, Einhorn TA. The bone organ system: form and function. In: Marcus R, Feldman D, Nelson DA, Rosen CJ, editors. Osteoporosis. 3rd ed. Burlington, MA: Elsevier Academic Press; 2008. p. 3–25.

[36] Tremollieres FA, Pouilles JM, Ribot C. Vertebral postmenopausal bone loss is reduced in overweight women: a longitudinal study in 155 early postmenopausal women. J Clin Endocrinol Metab 1993;77:683–6.

[37] Palacios C. The role of nutrients in bone health, from A to Z. Crit Rev Food Sci Nutr 2006;46:621–8.

[38] Tortoriello DV, McMinn J, Chua SC. Dietary-induced obesity and hypothalamic infertility in female DBA/2J mice. Endocrinology 2004;145:1238–47.

[39] Relling DP, Esberg LB, Fang CX, Johnson WT, Murphy EJ, Carlson EC, Saari JT, Ren J. High-fat diet-induced juvenile obesity leads to cardiomyocyte dysfunction and upregulation of Foxo3a transcription factor independent of lipotoxicity and apoptosis. J Hypertens 2006;24:549–61.

[40] Novack DV, Teitelbaum SL. The osteoclast: friend or foe? Annu Rev Pathol 2008;3:457–84.

[41] Cao J, Venton L, Sakata T, Halloran BP. Expression of RANKL and OPG correlates with age-related bone loss in male C57BL/6 mice. J Bone Miner Res 2003;18:270–7.

[42] Shoelson SE, Herrero L, Naaz A. Obesity, inflammation, and insulin resistance. Gastroenterology 2007;132:2169–80.

[43] Wellen KE, Hotamisligil GS. Obesity-induced inflammatory changes in adipose tissue. J Clin Invest 2003;112:1785–8.

[44] Boyle WJ, Simonet WS, Lacey DL. Osteoclast differentiation and activation. Nature 2003;423:337–42.

[45] Khosla S. Minireview: the OPG/RANKL/RANK system. Endocrinology 2001;142:5050–5.

[46] Lacey DL, Timms E, Tan HL, Kelley MJ, Dunstan CR, Burgess T, Elliott R, Colombero A, Elliott G, Scully S, Hsu H, Sullivan J, Hawkins N, Davy E, Capparelli C, Eli A, Qian YX, Kaufman S, Sarosi I, Shalhoub V, Senaldi G, Guo J, Delaney J, Boyle WJ. Osteoprotegerin ligand is a cytokine that regulates osteoclast differentiation and activation. Cell 1998;93:165–76.

[47] Simonet WS, Lacey DL, Dunstan CR, Kelley M, Chang MS, Luthy R, Nguyen HQ, Wooden S, Bennett L, Boone T, Shimamoto G, DeRose M, Elliott R, Colombero A, Tan HL, Trail G, Sullivan J, Davy E, Bucay N, Renshaw-Gegg L, Hughes TM, Hill D, Pattison W, Campbell P, Sander S, Van G, Tarpley J, Derby P, Lee R, Boyle WJ. Osteoprotegerin: a novel secreted protein involved in the regulation of bone density. Cell 1997;89:309–19.

[48] Kong YY, Yoshida H, Sarosi I, Tan HL, Timms E, Capparelli C, Morony S, Oliveira-dos-Santos AJ, Van G, Itie A, Khoo W, Wakeham A, Dunstan CR, Lacey DL, Mak TW, Boyle WJ, Penninger JM. OPGL is a key regulator of osteoclastogenesis, lymphocyte development and lymph-node organogenesis. Nature 1999;397:315–23.